Acta Crystallographica Section D
Biological Crystallography
ISSN 0907-4449

High-resolution structure of recombinant *Trichomonas vaginalis* thioredoxin

Jorge Iulek,[a,b] Magnus S. Alphey,[b] Gareth D. Westrop,[c] Graham H. Coombs[c] and William N. Hunter[b]*

[a]Department of Chemistry, Biotechnology Center, State University of Ponta Grossa, Ponta Grossa, Paraná, Brazil, [b]Division of Biological Chemistry and Molecular Microbiology, School of Life Sciences, University of Dundee, Dundee DD1 5EH, Scotland, and [c]Division of Infection and Immunity, Institute of Biomedical and Life Sciences, University of Glasgow, Glasgow G12 8QQ, Scotland

Correspondence e-mail: w.n.hunter@dundee.ac.uk

Received 16 September 2005
Accepted 30 November 2005

PDB Reference: thioredoxin, 2f51, r2f51sf.

The structure of thioredoxin from the anaerobic organism *Trichomonas vaginalis* (*Tv*Trx) has been determined at 1.9 Å resolution. The structure is that of a typical thioredoxin: a five-stranded β-sheet structure with two α-helices on either side. The active site of the protein carries a Trp-Cys-Gly-Pro-Cys motif, residues 34–38, at the N-terminus of an α-helix (α2). The cysteine residues in this motif form a redox-active disulfide necessary for thioredoxin activity. With high-resolution data available, it was possible to model numerous amino-acid side chains in alternate conformations and this includes the redox-active disulfide cysteine residues. The sample was initially in the oxidized state and the use of X-rays from an intense third-generation synchrotron source resulted in partial photoreduction of this labile redox centre. Comparisons with previously determined thioredoxin structures indicate that *Tv*Trx is most similar to the human homologue, although the insertion of three residues between strands β4 and β5 makes the corresponding turn longer and more flexible in *Tv*Trx. In addition, three significant amino-acid differences are identified on the protein surfaces near to the active-site Cys35. These residues may contribute to the interactions that specific thioredoxins form with their cognate physiological partners.

1. Introduction

The parasitic protozoon *Trichomonas vaginalis* is responsible for the sexually transmitted human disease trichomoniasis when infection of the genital tract is established (Petrin *et al.*, 1998). This flagellate protozoon is specialized to live under anaerobic conditions, yet has to cope with exposure to oxygen and also, arising from metabolism, to oxidative stress. Most organisms are dependent on the redox-active tripeptide glutathione (γ-Glu-Cys-Gly) as the major antioxidant/sulfhydryl buffer that is maintained in the reduced form by the NADPH-dependent flavoenzyme glutathione reductase (Krauth-Siegel *et al.*, 2005). Trichomonads apparently lack glutathione, glutathione-dependent peroxidase and catalase activities (Ellis *et al.*, 1994; Coombs *et al.*, 2004) and the amino acid cysteine may substitute for glutathione and carry out some of the protective functions against reactive oxygen species that are normally associated with that tripeptide.

Trichomonads depend upon NADH/NADPH oxidases to limit oxidative damage to their hydrogenosomes (Linstead & Bradley, 1988). One product of NADPH oxidase, however, is reactive hydrogen peroxide, the level of which has to be controlled. A recent study has identified the components of a thioredoxin-linked peroxiredoxin antioxidant system, similar to that found in many other organisms, in *T. vaginalis*, which is likely to do just that (Coombs *et al.*, 2004). The proteins involved are thioredoxin (Trx), thioredoxin reductase (TrxR) and a 2-Cys peroxiredoxin called thioredoxin peroxidase (TrxP), which together form a peroxidase cascade able to detoxify potentially damaging reactive oxygen species, including peroxides. Thioredoxin contributes to this protective function by shuttling reducing equivalents from TrxR to TrxP. Of note is the observation that Trx activity is increased when the parasites are exposed to elevated levels of oxygen or to a medium lacking ascor-

Table 1
Crystallographic statistics.

Values in parentheses represent the highest resolution bin of width approximately 0.06 Å.

Space group	*P*1
Unit-cell parameters (Å, °)	a = 33.88, b = 33.92, c = 50.50, α = 106.2, β = 109.0, γ = 91.7
Resolution range (Å)	32.29–1.90
No. of observed/unique reflections	74139/13709
Refined mosaicity (°)	1.5
Completeness of data (%)	90.0 (76.6)
$R_{\rm merge}$ (%)	3.8 (7.4)
$\langle I/\sigma(I)\rangle$	14.3 (9.2)
$R_{\rm cryst}$ (%)	14.7 (14.9)
$R_{\rm free}$ (%)	19.7 (23.7)
R.m.s.d. from ideal values, bond lengths (Å)	0.009
R.m.s.d. from ideal values, bond angles (°)	1.148
Ramachandran plot analysis	
Residues in most favoured regions (%)	94.3
Residues in additional allowed regions (%)	5.7

bate, indicating a direct and correlated response to oxidative stress (Coombs *et al.*, 2004).

Thioredoxins are not only involved in this type of peroxidase cascade, but are also implicated in numerous biological events where regulation of protein function and signalling processes can be achieved by thiol redox control (Arner & Holmgren, 2000; Buchanan & Balmer, 2005; Raina & Missiakas, 1997). These include regulation of transcription (Kontou *et al.*, 2004) and a molecular-chaperone function (Kern *et al.*, 2003; Raina & Missiakas, 1997).

We have undertaken the characterization of the structure–function relationships of proteins involved in regulating oxidative stress in protozoan parasites (see, for example, Alphey *et al.*, 2003) and have initiated crystallographic studies on *T. vaginalis* proteins. Here, we report the high-resolution crystal structure of *Tv*Trx and compare it with other thioredoxins, in particular the human host thioredoxin *Hs*Trx.

2. Materials and methods

2.1. Cloning, expression and purification

The *trx* gene was identified in an expressed sequence-tag database for *T. vaginalis*, cloned and inserted into the expression vector pET21a+ (Novagen) to create the plasmid pBP1, which was then introduced into *Escherichia coli* strain BL21(DE3) for protein production (Coombs *et al.*, 2004). The integrity of the gene sequence was confirmed on both strands (University of Glasgow DNA Sequencing Facility).

Single colonies of BL21(DE3) harbouring pBP1 were grown in Luria–Bertani medium, the expression of the recombinant protein was induced with 1 m*M* isopropyl thio-β-D-galactoside and, since the recombinant protein carries a C-terminal hexahistidine tag, it was purified using Ni^{2+}–NTA agarose (Qiagen) on a BioCad FPLC system. Protein concentration was determined using a molar extinction coefficient of 13 700 M^{-1} cm^{-1} at 280 nm and the purity of the sample was assessed by SDS–PAGE and matrix-assisted laser desorption time-of-flight mass spectrometry. The theoretical mass of the protein, native *Tv*Trx plus the tag, is 13 159 Da, while that observed by mass spectrometry was 13 191 Da. The difference between observed and calculated mass is 32 Da. We are confident about the integrity of the gene since it was confirmed by DNA sequencing and we did not observe any electron density during the analysis to suggest covalent modification of the protein or the presence of any ligand that might account for an increase in weight. The yield of purified protein was in excess of 30 mg per litre of bacterial cell culture; the protein was concentrated to 4 mg ml^{-1} in 100 m*M* sodium phosphate pH 7.0 and stored at 277 K.

2.2. Crystallization, diffraction data collection and processing

Crystals were obtained in hanging drops consisting of 1 µl protein solution and 1 µl reservoir solution (25% PEG 4000, 60 m*M* ammonium sulfate and 100 m*M* sodium acetate pH 4.9) equilibrated against 250 µl reservoir solution at 293 K. Needles grew in several weeks.

A single crystal (0.2 × 0.05 × 0.05 mm) was mounted in a nylon loop (Hampton Research) and cooled to 100 K with gaseous nitrogen (Oxford Cryosystems). X-ray diffraction data extending to 1.9 Å resolution were measured on an ADSC Q4 CCD detector using station ID14-EH2 at the European Synchrotron Radiation Facility, with the wavelength set at 0.9330 Å. The crystal-to-detector distance was 175 mm and 101 sequential images were recorded with an oscillation angle of 2°. Data were processed using *DENZO*/*SCALEPACK* (Otwinowski & Minor, 1997) and relevant statistics are presented in Table 1. Initial autoindexing calculations on the first images indicated the monoclinic space group *C*2 and suggested an angular range that would provide a complete data set. We measured slightly more than suggested, which was fortuitous because subsequently during data processing it was revealed that the space group is in fact *P*1.

2.3. Molecular replacement, model building and refinement

A homology model of *Tv*Trx was constructed with the program *MODELLER* (Sali & Blundell, 1993) using as the template an *E. coli* Trx structure (PDB code 2tir; Nikkola *et al.*, 1993). Molecular-replacement calculations (*Phaser*; McCoy *et al.*, 2005) were performed using data in the resolution range 32.2–1.90 Å. To minimize model bias, simulated annealing using the maximum-likelihood method was performed, followed by coordinate and thermal parameter refinement using *CNS* (Brünger *et al.*, 1998). The model was finally refined using *REFMAC*5 (Murshudov *et al.*, 1997), including TLS (translation/libration/screw-rotation) parameters. Non-crystallographic symmetry (NCS) restraints were not employed in this analysis. Visualization of electron density and difference density maps together with model manipulation were carried out using the program *Coot* (Emsley & Cowtan, 2004). The program *ARP_waters* (Perrakis *et al.*, 1999) was used to locate water molecules based on $2m|F_{\rm o}| - D|F_{\rm c}|$ and $m|F_{\rm o}| - D|F_{\rm c}|$ maps (where, for each reflection, m is the figure of merit, $F_{\rm o}$ and $F_{\rm c}$ represent observed and calculated structure factors, respectively, and D is the estimate of the error in the partial structure from coordinate errors; Read, 1986). Searches were carried out seeking to identify potential ions and ligands that might have been present from the protein purification, crystallization and cryoprotection procedures. These searches used *WASP* (Nayal & Di Cera, 1996), *XPAND* (G. J. Kleywegt, Uppsala University, Uppsala, Sweden, personal communication) and facilities embedded in *Coot*, but no additional ligands were identified. The refinement was concluded when no significant changes in $R_{\rm cryst}$ and $R_{\rm free}$ were observed and when inspection of the difference density map did not suggest any further additions/deletions or corrections to the model. Details are given in Table 1.

2.4. Structural comparison

The model of *Tv*Trx was submitted to the *DALI* server (Holm & Park, 2000; Holm & Sander, 1993) to determine the structural overlays with entries in the PDB (Berman *et al.*, 2002).

3. Results and discussion

3.1. Structure determination

Crystals of recombinant *Tv*Trx are triclinic, space group *P*1, with unit-cell parameters a = 33.88, b = 33.92, c = 50.49 Å, α = 106.2, β = 109.0, γ = 91.7°. The asymmetric unit contains two molecules. Molecular-replacement calculations identified two clear solutions, which after rigid-body refinement resulted in an $R_{\rm cryst}$ of 40.0% and electron-density maps of excellent quality. Subsequent refinement produced a model comprising 222 amino-acid residues (two protein chains, numbered 2–112 each) and 326 water molecules. The electron density for most of the structure was clearly interpretable (not shown), except for residues at the N-terminus of each molecule and also the region between residues 86–89, which corresponds to a flexible surface loop. A total of 38 residues have been modelled in alternate conformations; this approach produced an excellent fit of the model to the electron-density and difference density maps and improved the crystallographic residuals significantly. Included in these residues are the redox-active disulfides, which displayed a mixed population of reduced and oxidized states (discussed later). There were 14 side chains for which no convincing electron density was observed and although the atoms are included in the model, they were assigned a minimum occupancy of 0.1. This meant that the atoms did not contribute significantly to the calculated structure factors, but allowed the refinement program to maintain good geometry for these side chains. The crystallographic residuals and geometry of the model are acceptable for a high-resolution analysis, with all residues in either the most favoured or allowed regions of the Ramachandran plot (Table 1). An overlay of the two molecules in the asymmetric unit gives r.m.s.d. values of 0.44 Å for all C^{α} positions, 0.53 for main-chain atoms and 1.15 Å for all atoms common to each molecule. This high level of agreement observed in the absence of NCS restraints indicates that since the molecules are so similar it is only necessary to detail one.

The initial indexing suggested a monoclinic space group, *C*2. However, during data processing it became apparent that the space group was actually *P*1 since the agreement with predicted reflection positions gradually deteriorated to an extent that integration was not possible. The program *Pointless* (P. R. Evans, unpublished work), part of the *CCP*4 suite (Collaborative Computational Project, Number 4, 1994), was applied to investigate the Laue and space-group assignment. The lowest $R_{\rm meas}$ apart from *P*1 was indeed for *C*2, but with an improbably high $R_{\rm meas}$ of 52%. A self-rotation function was calculated and indicated a strong peak of NCS at φ = 90.3, ψ = 90.8, κ = 180.0°. This NCS twofold axis is nearly perpendicular to and near the mid-point of the *c* axis, parallel to the *ab* plane of the unit cell.

3.2. Overall structure

The structure of *Tv*Trx is that of a typical thioredoxin, belonging to the family of thioltransferases, as classified in the SCoP database (Murzin *et al.*, 1995). This fold corresponds to a core consisting of three layers $\alpha/\beta/\alpha$. The central β-sheet layer is composed of five strands, in the order $\beta1$-$\beta3$-$\beta2$-$\beta4$-$\beta5$ (Fig. 1). On either side of the β-sheet are the side chains that form an extensive hydrophobic core in the structure. On one side the residues that contribute are an alanine (68), two isoleucines (19, 58), a leucine (15), three phenylalanines (8, 30, 81), a threonine (56), a tyrosine (72) and six valines (26, 28, 60, 62, 74, 83). On the other side they are the aliphatic component of an asparagine (52), five isoleucines (5, 44, 48, 104, 108), five leucines (25, 27, 41, 45, 80), three phenylalanines (57, 82, 96) and a valine (55).

The active-site Trp-Cys-Gly-Pro-Cys motif (residues 34–38) is located between strand $\beta2$ and the N-terminus of helix $\alpha2$ (Fig. 1). The vicinal cysteine residues (Cys35 and Cys38) form a right-handed redox-active disulfide, a 14-membered ring system near the surface of the molecule, and are positioned beneath an overhanging Trp34. Cys35 is solvent-accessible and forms hydrogen bonds with two water molecules. These water molecules are likely to mark the position

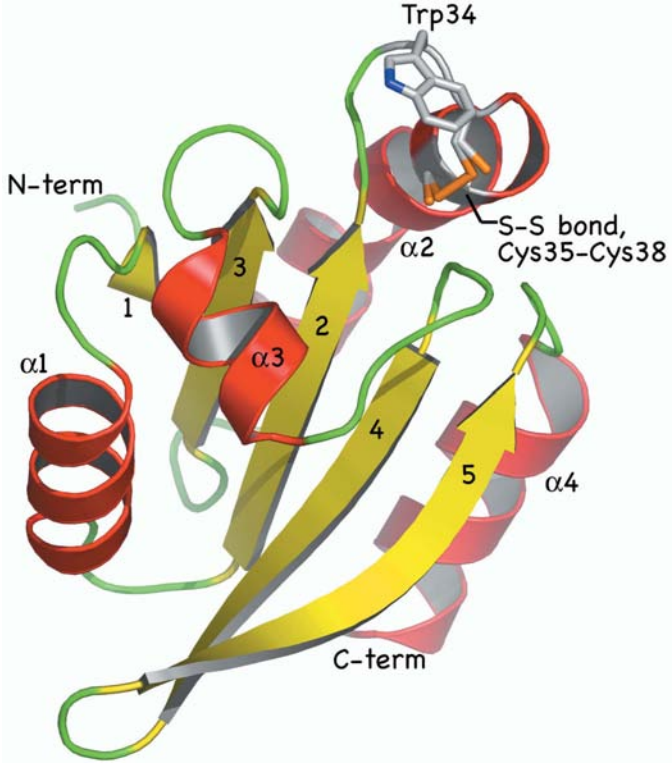

Figure 1
Ribbon diagram depicting the secondary structure and fold of *Tv*Trx. α-Helices are red, β-strands yellow and segments of coil green. Trp34, Cys35 and Cys38 side chains, which mark the redox centre, are presented as sticks coloured according to atomic position, where N is blue, C grey and S orange. Figs. 1, 2 and 3(*a*) were prepared using *PyMOL* (DeLano, 2002).

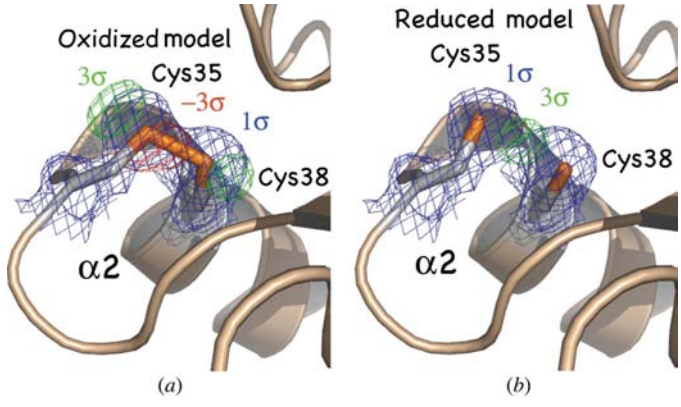

Figure 2
Evidence for a mixed dithiol–disulfide involving Cys35–Cys38. (*a*) The electron-density map at a 1σ level is depicted as blue chicken-wire. The positive and negative difference densities are shown as green and red chicken-wire, respectively, both at a 3σ level. The phases used for the calculation of these maps are derived from a model in which the Cys35–Cys38 disulfide was given full occupancy. (*b*) Here, depicted in similar fashion to (*a*), the reduced form of the Cys35–Cys38 pair was given full occupancy.

where redox partners bind (not shown). On the other side of Cys35 SG, a hydrogen bond is donated from the main-chain amide of Cys38. Trp34 NE1 accepts a hydrogen bond donated from Asp63 OD2, which is likely to be protonated, and this helps to position the tryptophan over the methyl group of Ala32 (not shown). The tryptophan lid over the redox disulfide, a ubiquitous feature of the thioredoxin superfamily, is able to adopt different positions with respect to the redox disulfide, as noted in a mutant *E. coli* Trx (Nikkola *et al.*, 1993), in a chloroplast Trx (Capitani *et al.*, 2000) and in the trypanosomatid protein called tryparedoxin (Tryx). This tryptophan is a key residue in docking interactions of Trx and Tryx with redox partners (Alphey *et al.*, 2003).

The electron-density and difference density maps indicated that the redox disulfide was partially reduced (Fig. 2) and therefore the side chains of Cys35 and Cys38 have been modelled in alternate conformations. In molecule *A* the occupancies of the oxidized and reduced forms are 0.6 and 0.4, respectively, while in molecule *B* they are both set to 0.5. These occupancies were not refined but rather tested and the most appropriate combination selected on the basis of thermal parameter refinement. Previous studies on Trx show that in crude cell-free extracts up to 90% of the protein is oxidized (Holmgren & Fagerstedt, 1982). We assume that the protein was in the oxidized state as the sample that was crystallized was not exposed to reducing agents after purification and spent several weeks in crystallization conditions. The diffraction data were recorded using an intense third-generation synchrotron-radiation source on an undulator beamline; this fact combined with the length of time required to obtain a complete data set (owing to the low symmetry of the sample) and the small size of the crystal lead us to propose that the high-energy X-ray dose had been sufficient to partially photoreduce the labile disulfide. This observation is consistent with previous studies on the structurally related Tryx, where increasing X-ray doses were applied to crystals and used to generate the reduced protein *in situ* (Alphey *et al.*, 2003). In common with other studies (Capitani *et al.*, 2000), we do not observe large conformational changes that can be attributed to a change in the redox state of the disulfide. In their study, Capitani and coworkers studied a spinach chloroplast Trx, but in contrast to our work they first measured data on the reduced form of the protein. Then, over a period of almost 2 d with an in-house X-ray source and crystals maintained at 277 K, they were able to isolate a data set from a crystal in which the disulfide had reformed without any large perturbation to the active site. Given that irrespective of whether the structures being used for comparisons were determined first in reduced or oxidized state all structures overlay well, as described in the next section, then it would appear that only a minor highly localized perturbation of the Trx structure accompanies the change in oxidation state.

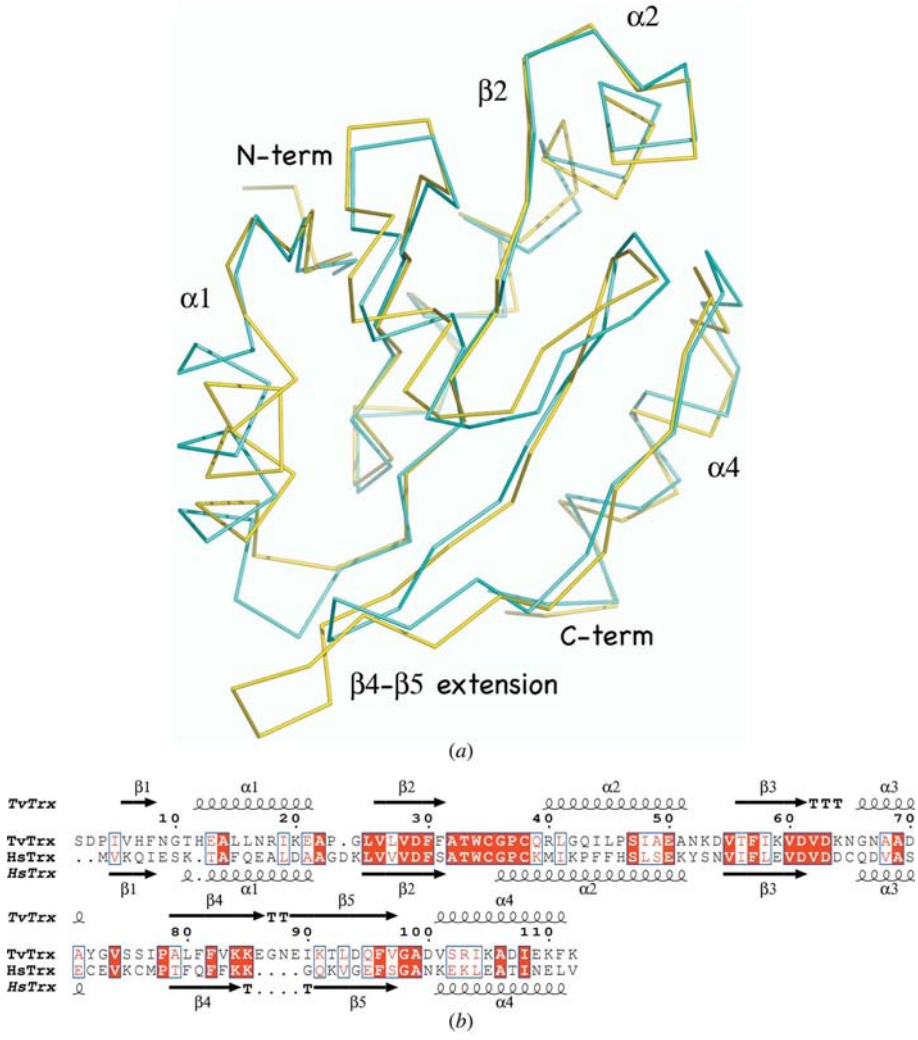

Figure 3
Comparison of *Tv*Trx and *Hs*Trx. (*a*) C$^{\alpha}$ trace of *Tv*Trx (yellow) superposed on *Hs*Trx (cyan). The orientation for *Tv*Trx is the same as used in Fig. 1. (*b*) Sequence comparison based on the structural alignment generated by the program *ESPript* (Gouet *et al.*, 2003). Residues denoted as white letters on red background are strictly conserved between the two proteins; residues given as red letters on a white background are homologous. The assigned secondary structure is given for each protein.

3.3. Comparison with human thioredoxins

Thioredoxins are highly conserved with sequence identities in the range 27–70% across species (Eklund *et al.*, 1991) and alignments of topologically equivalent C$^{\alpha}$ positions of the eight Trx structures in the PDB give r.m.s.d. values of between 1.6 and 2.0 Å (Peterson *et al.*, 2005). The sequence identity between *Tv*Trx and the cytosolic *Hs*Trx is 35% and superposition of these two structures gives an r.m.s.d. of 1.25 Å for 104 C$^{\alpha}$ atoms. The structures overlay well, with the only minor difference being an extension of three residues (Gly87-Asn88-Glu89) in *Tv*Trx (Fig. 3*a*). This is on the surface of the protein in the turn linking β4 with β5, distant from the active site of the protein. A structure-based sequence alignment of *Tv*Trx and *Hs*Trx is shown in Fig. 3(*b*).

Those residues that form the hydrophobic core of *Tv*Trx are in general well conserved in *Hs*Trx; for example 12 of the 30 residues listed earlier are strictly conserved and another eight are hydrophobic residues similar in size (Fig. 3*b*). Three rather different residues positioned in the thioredoxin core are Tyr72, Phe81 and Val83 of *Tv*Trx, which are replaced by Cys69, Gln78 and Phe80 in *Hs*Trx.

The surface of thioredoxin near to Cys35 is where partner proteins and metabolites interact. Here, we note three significant differences between the two proteins. In *Tv*Trx, Phe31, Gly42 and Lys59 are replaced by Ser28, Lys39 and Glu56, respectively, in *Hs*Trx (Fig. 3*b*). These differences could play important roles in determining the specificities of the individual thioredoxins, for although thioredoxins in general have similar overall structures, they possess quite distinct abilities to interact with protein partners. This includes the multiple thioredoxin isoforms observed within one organism. Small structural differences are thought to be important in enabling the proteins to perform their specific functions. Notably, thioredoxin reductase is one major partner of thioredoxin and yet the enzymes of *T. vaginalis* and human are fundamentally different in structure (Coombs *et al.*, 2004).

Structural studies of human cytosolic and mitochondrial Trx (Smeets *et al.*, 2005; Weichsel *et al.*, 1996) apparently show the presence of regulatory dimers. Although the crystal structure of *Tv*Trx presents two molecules in the asymmetric unit, there is no data to suggest that a dimer exists in solution and the arrangement of the molecules is in any case different from that observed in the mammalian protein structures.

In summary, as part of a project to characterize proteins involved in the regulation of oxidative stress in protozoan parasites we have determined the high-resolution structure of recombinant thioredoxin from *T. vaginalis*. The protein presents the typical thioredoxin fold. The redox-active disulfide, formed by Cys35–Cys38, has been partially photoreduced by the intense synchrotron radiation used in data collection. Comparisons using the *DALI* server (Holm & Park, 2000) identified *Hs*Trx as the closest structural homologue known. Comparison of residues in the vicinity of the redox-active disulfides has identified several of them on the surface of the structures that are likely to be involved in associations with cognate physiological partners and may be critical in determining the specificities of the thioredoxins.

JI thanks CAPES for fellowship number BEX 2000/04-0. WNH thanks The Wellcome Trust and Biotechnology and Biological Sciences Research Council (UK) for support. We gratefully acknowledge the provision of synchrotron beam time at the European Synchrotron Radiation Facility and thank their staff for support and also Dr P. Evans for a preprint concerning his useful program *Pointless*.

References

Alphey, M. S., Gabrielsen, M., Micossi, E., Leonard, G. A., McSweeney, S. M., Ravelli, R. B., Tetaud, E., Fairlamb, A. H., Bond, C. S. & Hunter, W. N. (2003). *J. Biol. Chem.* **278**, 25919–25925.
Arner, E. S. & Holmgren, A. (2000). *Eur. J. Biochem.* **267**, 6102–6109.
Berman, H. M., Battistuz, T., Bhat, T. N., Bluhm, W. F., Bourne, P. E., Burkhardt, K., Feng, Z., Gilliland, G. L., Iype, L., Jain, S., Fagan, P., Marvin, J., Padilla, D., Ravichandran, V., Schneider, B., Thanki, N., Weissig, H., Westbrook, J. D. & Zardecki, C. (2002). *Acta Cryst.* D**58**, 899–907.
Brünger, A. T., Adams, P. D., Clore, G. M., DeLano, W. L., Gros, P., Grosse-Kunstleve, R. W., Jiang, J.-S., Kuszewski, J., Nilges, N., Pannu, N. S., Read, R. J., Rice, L. M., Simonson, T. & Warren, G. L. (1998). *Acta Cryst.* D**54**, 905–921.
Buchanan, B. B. & Balmer, Y. (2005). *Annu. Rev. Plant Biol.* **56**, 187–220.
Capitani, G., Markovic Housley, Z., DelVal, G., Morris, M., Jansonius, J. N. & Schurmann, P. (2000). *J. Mol. Biol.* **302**, 135–154.
Collaborative Computational Project, Number 4 (1994). *Acta Cryst.* D**50**, 760–763.
Coombs, G. H., Westrop, G. D., Suchan, P., Puzova, G., Hirt, R. P., Embley, T. M., Mottram, J. C. & Müller, S. (2004). *J. Biol. Chem.*, **279**, 5249–5256.
DeLano, W. L. (2002). *The PyMOL Molecular Graphics System.* DeLano Scientific, San Carlos, CA, USA.
Eklund, H., Gleason, F. K. & Holmgren, A. (1991). *Proteins*, **11**, 13–28.
Ellis, J. E., Yarlett, N., Cole, D., Humphreys, M. J. & Lloyd, D. (1994). *Microbiology*, **140**, 2489–2494.
Emsley, P. & Cowtan, K. (2004). *Acta Cryst.* D**60**, 2126–2132.
Gouet, P., Robert, X. & Courcelle, E. (2003). *Nucleic Acids Res.* **31**, 3320–3323.
Holm, L. & Park, J. (2000). *Bioinformatics*, **16**, 566–567.
Holm, L. & Sander, C. (1993). *J. Mol. Biol.* **233**, 123–138.
Holmgren, A. & Fagerstedt, M. (1982). *J. Biol. Chem.* **257**, 6926–6930.
Kern, R., Malkim A., Holmgren, A. & Richarme, G. (2003). *Biochem. J.* **371**, 965–972.
Kontou, M., Will, R. D., Adelfalk, C., Wittig, R., Poustka, A., Hirsch-Kauffmann, M. & Schweiger, M. (2004). *Oncogene*, **23**, 2146–2152.
Krauth-Siegel, R. L., Bauer, H. & Schirmer, R. H. (2005). *Angew. Chem. Int. Ed.* **44**, 690–715.
Linstead, D. J. & Bradley, S. (1988). *Mol. Biochem. Parasitol.* **27**, 125–133.
McCoy, A. J., Grosse-Kunstleve, R. W., Storoni, L. C. & Read, R. J. (2005). *Acta Cryst.* D**61**, 458–464.
Murshudov, G. N., Vagin, A. A. & Dodson, E. J. (1997). *Acta Cryst.* D**53**, 240–255.
Murzin, A. G., Brenner, S. E., Hubbard, T. & Chothia, C. (1995). *J. Mol. Biol.* **247**, 536–540.
Nayal, M. & Di Cera, E. (1996). *J. Mol. Biol.* **256**, 228–234.
Nikkola, M., Gleason, F. K., Fuchs, J. A. & Eklund, H. (1993). *Biochemistry*, **32**, 5093–5098.
Otwinowski, Z. & Minor, W. (1997). *Methods Enzymol.* **276**, 307–326.
Perrakis, A., Morris, R. J. H. & Lamzin, V. S. (1999). *Nature Struct. Biol.* **6**, 458–463.
Peterson, F. C., Lytle, B. L., Sampath, S., Vinarov, D., Tyler, E., Shahan, M., Markley, J. L. & Volkman, B. F. (2005). *Protein Sci.* **14**, 2195–2200.
Petrin, D., Delgaty, K., Bhatt, R. & Garber, G. (1998). *Clin. Microbiol. Rev.* **11**, 300–317.
Raina, S. & Missiakas, D. (1997). *Annu. Rev. Microbiol.* **51**, 179–202.
Read, R. J. (1986). *Acta Cryst.* A**42**, 140–149.
Sali, A. & Blundell, T. L. (1993). *J. Mol. Biol.* **234**, 779–815.
Smeets, A., Evrard, C., Landtmeters, M., Marchand, C., Knoops, B. & Declercq, J.-P. (2005). *Protein Sci.* **14**, 2610–2621.
Weichsel, A., Gasdaska, J. R., Powis, P. & Montford, W. R. (1996). *Structure*, **4**, 735–751.